ANL/NDM-52

NEUTRON TOTAL AND SCATTERING CROSS SECTIONS OF ^{6}Li IN THE FEW MeV REGION

by

P. Guenther, A. Smith and J. Whalen

February 1980

Applied Physics Division
ARGONNE NATIONAL LABORATORY
9700 South Cass Avenue
Argonne, Illinois 60439
USA

NUCLEAR DATA AND MEASUREMENTS SERIES

The Nuclear Data and Measurements Series presents results of studies in the field of microscopic nuclear data. The primary objective is the dissemination of information in the comprehensive form required for nuclear technology applications. This Series is devoted to: a) measured microscopic nuclear parameters, b) experimental techniques and facilities employed in measurements, c) the analysis, correlation and interpretation of nuclear data, and d) the evaluation of nuclear data. Contributions to this Series are reviewed to assure technical competence and, unless otherwise stated, the contents can be formally referenced. This Series does not supplant formal journal publication but it does provide the more extensive information required for technological applications (e.g., tabulated numerical data) in a timely manner.

OTHER ISSUES IN THE ANL/NDM SERIES ARE:

ANL/NDM-1 Cobalt Fast Neutron Cross Sections-Measurement and Evaluation by P. T. Guenther, P. A. Moldauer, A. B. Smith, D. L. Smith and J. F. Whalen, July 1973.

ANL/NDM-2 Prompt Air-Scattering Corrections for a Fast-Neutron Fission Detector: $E_n \leq 5$ MeV by Donald L. Smith, September 1973.

ANL/NDM-3 Neutron Scattering from Titanium; Compound and Direct Effects by E. Barnard, J. deVilliers, P. Moldauer, D. Reitmann, A. Smith and J. Whalen, October 1973.

ANL/NDM-4 ^{90}Zr and ^{92}Zr; Neutron Total and Scattering Cross Sections by P. Guenther, A. Smith and J. Whalen, July 1974.

ANL/NDM-5 Delayed Neutron Data - Review and Evaluation by Samson A. Cox, April 1974.

ANL/NDM-6 Evaluated Neutronic Cross Section File for Niobium by R. Howerton, Lawrence Livermore Laboratory and A. Smith, P. Guenther and J. Whalen, Argonne National Laboratory, May 1974.

ANL/NDM-7 Neutron Total and Scattering Cross Sections of Some Even Isotopes of Molybdenum and the Optical Model by A. B. Smith, P. T. Guenther and J. F. Whalen, June 1974.

ANL/NDM-8 Fast Neutron Capture and Activation Cross Sections of Niobium Isotopes by W. P. Poenitz, May 1974.

ANL/NDM-9 Method of Neutron Activation Cross Section Measurement for E_n = 5.5-10 MeV Using the D(d,n)He-3 Reaction as a Neutron Source by D. L. Smith and J. W. Meadows, August 1974.

ANL/NDM-10 Cross Sections for (n,p) Reactions on ^{27}Al, $^{46,47,48}Ti$, $^{54,56}Fe$, ^{58}Ni, ^{59}Co and ^{64}Zn from Near Threshold to 10 MeV by Donald L. Smith and James W. Meadows, January 1975.

ANL/NDM-11 Measured and Evaluated Fast Neutron Cross Sections of Elemental Nickel by P. Guenther, A. Smith, D. Smith and J. Whalen, Argonne National Laboratory and R. Howerton, Lawrence Livermore Laboratory, July 1975.

ANL/NDM-12 A Spectrometer for the Investigation of Gamma Radiation Produced by Neutron-Induced Reactions by Donald L. Smith, April 1975.

ANL/NDM-13 Response of Several Threshold Reactions in Reference Fission Neutron Fields by Donald L. Smith and James W. Meadows, June 1975.

ANL/NDM-14 Cross Sections for the $^{66}Zn(n,p)^{66}Cu$, $^{113}In(n,n')^{113m}In$ and $^{115}In(n,n')^{115m}In$ Reactions from Near Threshold to 10 MeV by Donald L. Smith and James W. Meadows, July 1975.

ANL/NDM-15 Radiative Capture of Fast Neutrons in ^{165}Ho and ^{181}Ta by W. P. Poenitz, June 1975.

ANL/NDM-16 Fast Neutron Excitation of the Ground-State Rotational Band of ^{238}U by P. Guenther, D. Havel and A. Smith, September 1975.

ANL/NDM-17 Sample-Size Effects in Fast-Neutron Gamma-Ray Production Measurements: Solid-Cylinder Samples by Donald L. Smith, September 1975.

ANL/NDM-18 The Delayed Neutron Yield of ^{238}U and ^{241}Pu by J. W. Meadows January 1976.

ANL/NDM-19 A Remark on the Prompt-Fission-Neutron Spectrum of ^{252}Cf by P. Guenther, D. Havel, R. Sjoblom and A. Smith, March 1976.

ANL/NDM-20 Fast-Neutron-Gamma-Ray Production from Elemental Iron: $E_n \lesssim$ 2 MeV by Donald L. Smith, May 1976.

ANL/NDM-21 Note on the Experimental Determination of the Relative Fast-Neutron Sensitivity of a Hydrogenous Scintillator by A. Smith, P. Guenther and R. Sjoblom, June 1976.

ANL/NDM-22 Note on Neutron Scattering and the Optical Model Near A=208 by P. Guenther, D. Havel and A. Smith, September 1976.

ANL/NDM-23 Remarks Concerning the Accurate Measurement of Differential Cross Sections for Threshold Reactions Used in Fast-Neutron Dosimetry for Fission Reactors by Donald L. Smith, December 1976.

ANL/NDM-24 Fast Neutron Cross Sections of Vanadium and an Evaluated Neutronic File by P. Guenther, D. Havel, R. Howerton, F. Mann, D. Smith, A. Smith and J. Whalen, May 1977.

ANL/NDM-25 Determination of the Energy Scale for Neutron Cross Section Measurements Employing a Monoenergetic Accelerator by J. W. Meadows, January 1977.

ANL/NDM-26 Evaluation of the IN-115(N,N')IN-115M Reaction for the ENDF/B-V Dosimetry File by Donald L. Smith, December 1976.

ANL/NDM-27 Evaluated (n,p) Cross Sections of ^{46}Ti, ^{47}Ti and ^{48}Ti by C. Philis and O. Bersillon, Bruyeres-le-Chatel, France and D. Smith and A. Smith, Argonne National Laboratory, January 1977.

ANL/NDM-28 Titanium-II: An Evaluated Nuclear Data File by C. Philis, Centre d'Etudes de Bruyéres-le-Châtel, R. Howerton, Lawrence Livermore Laboratory and A. B. Smith, Argonne National Laboratory, June 1977.

ANL/NDM-29 Note on the 250 keV Resonance in the Total Neutron Cross Section of ^{6}Li by A. B. Smith, P. Guenther, D. Havel and J. F. Whalen, June 1977.

ANL/NDM-30 Analysis of the Sensitivity of Spectrum-Average Cross Sections to Individual Characteristics of Differential Excitation Functions by Donald L. Smith, March 1977.

ANL/NDM-31 Titanium-I: Fast Neutron Cross Section Measurements by P. Guenther, D. Havel, A. Smith and J. Whalen, May 1977.

ANL/NDM-32 Evaluated Fast Neutron Cross Section of Urnaium-238 by W. Poenitz, E. Pennington, and A. B. Smith, Argonne National Laboratory and R. Howerton, Lawrence Livermore Laboratory, October 1977.

ANL/NDM-33 Comments on the Energy-Averaged Total Neutron Cross Sections of Structural Materials by A. B. Smith and J. F. Whalen, June 1977.

ANL/NDM-34 Graphical Representation of Neutron Differential Cross Section Data for Reactor Dosimetry Applications by Donald L. Smith, June 1977.

ANL/NDM-35 Evaluated Nuclear Data File of Th-232 by J. Meadows, W. Poenitz, A. Smith, D. Smith and J. Whalen, Argonne National Laboratory and R. Howerton, Lawrence Livermore Laboratory, February 1978.

ANL/NDM-36 Absolute Measurements of the $^{233}U(n,f)$ Cross Section Between 0.13 and 8.0 MeV by W. P. Poenitz, April 1978.

ANL/NDM-37 Neutron Inelastic Scattering Studies for Lead-204 by D. L. Smith and J. W. Meadows, December 1977.

ANL/NDM-38 The Alpha and Spontaneous Fission Half-Lives of ^{242}Pu by J. W. Meadows, December 1977.

ANL/NDM-39 The Fission Cross Section of ^{239}Pu Relative to ^{235}U from 0.1 to 10 MeV by J. W. Meadows, March 1978.

ANL/NDM-40 Statistical Theory of Neutron Nuclear Reactions by P. A. Moldauer, February 1978.

ANL/NDM-41 Energy-Averaged Neutron Cross Sections of Fast-Reactor Structural Materials by A. Smith, R. McKnight and D. Smith, February 1978.

ANL/NDM-42 Fast Neutron Radiative Capture Cross Section of ^{232}Th by W. P. Poenitz and D. L. Smith, March 1978.

ANL/NDM-43 Neutron Scattering from ^{12}C in the Few-MeV Region by A. Smith, R. Holt and J. Whalen, September 1978.

ANL/NDM-44 The Interaction of Fast Neutrons with ^{60}Ni by A. Smith, P. Guenther, D. Smith and J. Whalen, January 1979.

ANL/NDM-45 Evaluation of $^{235}U(n,f)$ between 100 KeV and 20 MeV by W. P. Poenitz, July 1979.

ANL/NDM-46 Fast-Neutron Total and Scattering Cross Sections of ^{107}Ag in the MeV Region by A. Smith, P. Guenther, G. Winkler and J. Whalen, January 1979.

ANL/NDM-47 Scattering of MeV Neutrons from Elemental Iron by A. Smith and P. Guenther, March 1979.

ANL/NDM-48 ^{235}U Fission Mass and Counting Comparison and Standardization by W. P. Poenitz, J. W. Meadows and R. J. Armani, May 1979.

ANL/NDM-49 Some Comments on Resolution and the Analysis and Interpretation of Experimental Results from Differential Neutron Measurements by Donald L. Smith, November 1979.

ANL/NDM-50 Prompt-Fission-Neutron Spectra of ^{233}U, ^{235}U, ^{239}Pu and ^{240}Pu Relative to that of ^{252}Cf by A. Smith, P. Guenther, G. Winkler and R. McKnight, September 1979.

ANL/NDM-51 Measured and Evaluated Neutron Cross Sections of Elemental Bismuth by A. Smith, P. Guenther, D. Smith and J. Whalen, April 1980.

ANL/NDM-52 Neutron Total and Scattering Cross Sections of ^{6}Li in the Few MeV Region by P. Guenther, A. Smith and J. Whalen, February 1980.

TABLE OF CONTENTS

LIST OF FIGURES

LIST OF FIGURES (Contd.)

LIST OF TABLES

NEUTRON TOTAL AND SCATTERING CROSS SECTIONS OF ^{6}Li IN THE FEW MeV REGION*

by

P. Guenther, A. Smith and J. Whalen
Argonne National Laboratory
Argonne, Illinois 60439

ABSTRACT

Neutron total cross sections of ^{6}Li are measured from ~0.5 to ~4.8 MeV at intervals of $\lesssim$10 keV. Neutron differential elastic-scattering cross sections are measured from 1.5 to 4.0 MeV at $\gtrsim$10 scattering angles and at incident-neutron intervals of $\lesssim$100 keV. Neutron differential inelastic-scattering cross sections are measured in the incident-energy range 3.5 to 4.0 MeV. The experimental results are extended to lower energies using measured neutron total cross sections recently reported elsewhere by the authors. The composite experimental data (total cross sections from 0.1-4.8 MeV and scattering cross sections from 0.22-4.0 MeV) are interpreted in terms of a simple two-level R-matrix model which describes the observed cross sections and implies the reaction cross section in unobserved channels; notably the (n;α)t reaction (Q = 4.783 MeV). The experimental and calculational results are compared with previously reported results as summarized in the ENDF/B-V evaluated nuclear data file.

*This work supported by the U. S. Department of Energy.

I. Introduction

Despite its probable simplicity, the nuclear structure underlying the n + ^{6}Li reaction in the few-MeV region is not well known (1) and the understanding of the corresponding cross sections is only fragmentary (2). Neutron and alpha-particle channels are open at thermal energies and the respective cross sections imply a large $\ell = 0$ component. Yet, no corresponding $\ell = 0$ resonance has been explicitly identified at relevant energies. A large 5/2 - resonance dominates reactions in the few-hundred keV region. At higher energies the contributing resonance structure is broad and ill-defined and a number of channels are open at an incident neutron energy of 4 to 5 MeV. The (n;α) cross section follows an essentially 1/v behavior from thermal to ~100 keV and is widely used as a reference standard in experimental fast-neutron studies (3). The ^{6}Li(n,α)t reaction plays a prominent part in tritium production in many fusion-energy concepts. Thus, from the point of view of nuclear structure, neutron standards and nuclear applications the n + ^{6}Li reaction in the few-MeV region is of interest. Despite this wide relevance, the reaction is not well known.

A joint Bureau Central de Mesures Nuclaires (BCMN) and Argonne National Laboratory (ANL) study has address the n + ^{6}Li reaction over a several year period. Two, lower-energy, experimental portions of this work have been reported (4,5). The final higher-energy portion, extending to ~4.8 MeV, and an interpretation of the whole is presented in this paper. Sections II and III address the higher energy portions of the experimental measurements. Section IV presents the composite experimental results extending from ~0.1 to 4.8 MeV with emphasis on the higher-energy region. Section V discusses the interpretation of the entire experimental data base and its implications. The remarks of Section VI summarize the experimental and calculational aspects of the program.

II. Samples

The samples employed in the ANL neutron total cross section measurements (0.5 to 4.75 MeV) and the ANL differential neutron scattering measurements (1.5 to 4.0 MeV) are defined below. Samples employed in other aspects of the measurement program are defined in Refs. 4 and 5.

The two samples fabricated at Argonne National Laboratory (ANL-1, ANL-2) were cast of metallic lithium enriched to 95.4 atom-percent in ^{6}Li. The assay of the stock material indicated no significant chemical impurities. The molten-lithium metal was poured, under an argon atmosphere, into ≈0.025 cm. thick cylindrical stainless steel containers 2 cm. in diameter and 2 cm. long. The containers were sealed using electron-beam-welding techniques. Identical empty containers were concurrently fabricated. After fabrication the samples were inspected using radiographic procedures. No voids were detected but a small miniscus was noted apparently as a result of the casting procedures. Mean atomic densities were calculated from the weights of empty and filled containers and the respective dimensions. The resulting densities differed by about 3 percent, possibly reflecting some porosity or simply slight variations in casting procedures.

The ANL-1 and -2 samples were primarily designed for scattering measurements. Uncertainties, such as those due to porosity and miniscuses, would have little effect on scattering-cross-section results; they were a concern in total cross section measurements which were sensitive to precise determinations of sample thickness. Both ANL samples were too thin for good total cross section results in the MeV range so they were used in tandem for such measurements. The single thicknesses were suitable for measurements near the peak of the 250 keV resonance and they were used singly in measurements of total cross sections in this region as outlined in Ref. 5.

Few-MeV total-cross-section measurements obtained with the ANL-1 and -2 samples were compared with those obtained with a larger ($\approx$5 cm. thick) sample fabricated at ANL. The agreement was with $\lesssim$2 percent but this larger sample was also cast into a container and thus subject to some of the same uncertainties as ANL-1 and -2. A precisely machined 5.538 cm. thick sample was obtained on loan from BCMN. This reference sample was enriched to 95.63 atom-percent in ^{6}Li and the atomic density was reported to precisions of better than 0.1 percent. The fabrication of the BCMN sample and the parameter determinations were completely independent of those of the ANL samples. Total cross sections obtained with the BCMN and two ANL samples were carefully compared throughout the region of the 250 keV resonance, as outlined in Ref. 5, where the respective transmissions were optimized for best statistical accuracies. The results obtained with the ANL-1 sample were indistinguishable, to within the statistical uncertainties of $\lesssim$1 percent, from those obtained with the BCMN sample. The results obtained with the ANL-2 sample were about 3 percent different from the above common value. Very careful and highly redundant measurements in the MeV region tended to show the same discrepancy though the ANL samples were too thin when used singly in this energy region to give very precise total cross section results. In view of the above comparisons, the BCMN and ANL-1 samples were designated as the "primary" samples and total cross section results were corrected to their densities. The corrections applied only to results involving ANL-2. In the total-cross-section results, the corrections were straight-forward and small ($\approx$2 percent). The total-cross-section corrections for ANL-2 may reflect porosities or the miniscus rather than differences in sample masses. Thus the same corrections are not, a priori, applicable to the scattering results. The scattering corrections were obtained from detailed comparisons of scattering results in the few MeV range obtained using ANL-1 and -2 samples. Such comparisons are difficult and the resulting correction factors ($\approx$2 percent) were generally a small part of the overall random uncertainties in the measured scattering cross sections, thus they need not be very accurately known.

As noted above, all samples contained $\approx$4.5 atom-percent of ^{7}Li. All measured values were corrected for this ^{7}Li contaminant using the ^{7}Li cross sections as given in ENDF/B-IV (6).

III. Experimental Methods

In this Section the methods applicable to the determination of neutron total cross sections from 0.5 to 4.75 MeV and scattering cross sections from 1.5 to 4.0 MeV are outlined. The methods employed at lower energies are outlined in Ref. 5.

A. Broad-Resolution Total Cross Section Measurements in the MeV Region

The broad-resolution total cross section measurements in the MeV region were made using the computer-controlled apparatus at the Argonne Fast Neutron Generator (7). Nanosecond bursts of approximately monoenergetic neutrons were obtained using the $^{7}Li(p;n)^{7}Be$ reaction (8). The targets were prepared by vacuum evaporation of lithium metal on to a tantalum backing to a thickness giving the desired incident-neutron energy spreads of ≈30 to 50 keV. The neutron source was surrounded by a massive water filled shield. A 1 m long copper collimator was arranged in this shield so as to provide an ≈1 cm diameter neutron beam at a zero-degree reaction angle. A sample holder was placed ≈10 cm from the collimator exit. This sample holder consisted of a wheel that "stepped" the samples, voids and empty containers through the beam. Neutrons were incident upon the bases of the cylindrical samples. Each sample was in the beam for 500 msec and data storage was correlated with sample position in an on-line digital computer. The sample cycle times were sufficiently fast to avoid independent monitoring of source intensity. The detector consisted of a hydrogeneous scintillator placed ≈3 m from the sample wheel on the beam axis. Conventional pulsed-beam time-of-flight techniques were used to record the velocity spectrum of neutrons arriving at the detector. The prominent peak in the spectra corresponding to the primary $^{7}Li(p;n)^{7}Be$ neutron group was integrated and corrected for background effects as deduced from regions on either side of the peak. The observed velocity resolution was sufficient to resolve this primary group from the secondary $^{7}Li(p;n)^{7}Be^{*}$ neutron group and from energy-degraded neutrons that might have scattered in the collimator-shield materials. Sample transmissions and associated uncertainties were continuously calculated in real-time and measurements were continued until pre-determined statistical accuracies were achieved. Total neutron cross sections were then deduced from the observed neutron transmissions in a straight-forward manner (9).

Attention was given to possible experimental perturbations. A real-time clock was inserted in the detection system in order to precisely determine small dead-time corrections and these were further verified by changing source intensities by factors of four. Calculational estimates showed in-scattering corrections to be negligible and this was supportgd by the consistency of cross-section results obtained with approximately a factor of two different transmissions.

The sample wheel contained the ^{6}Li samples, corresponding empty containers, samples of carbon, silicon and sulphur and a void. The energy scale was determined to within ± 8 keV by the control of the proton beam and verified by using the well-known energies of prominent carbon, silicon and sulphur resonances (10). In addition, the carbon total cross sections were determined. Away from carbon resonances they were in good agreement ($\lesssim$1 percent) with previously reported values and thus verified the fidelity of the apparatus (11). The ANL ^{6}Li samples were too thin to obtain statistically good cross sections in this energy range when used singly; therefore they were arranged in tandem (excepting sample and instrument-verification tests) to obtain a total sample thickness of ≈4 cm. The BCMN sample was used singly, providing a sample thickness of ≈5.5 cm.

B. Differential Neutron Scattering Measurements

The $^{7}Li(p;n)^{7}Be$ reaction was employed as a neutron source throughout the scattering measurements. The incident-neutron energy scale was known to ≈10 keV. The incident neutron energy spread was 15 to 30 keV depending upon the particular measurement. Generally, the energy spread was smaller at the higher incident energies. The use of the Li source reaction was identical to that outlined above in the context of the total cross section measurements. The primary monitor for neutron-source intensity was an independent time-of-flight system arranged so as to be insensitive to neutrons other than those directly from the primary $^{7}Li(p;n)^{7}Be$ source. Uncertainties associated with monitoring the source intensity were generally small; less that 1 percent.

All the differential scattering measurements were made using the fast time-of-flight technique and the Argonne 10-angle time-of-flight system (12). Measurements were made at ten or more scattering angles distributed between ≈20 and 160 deg. The relative angular placement of the detectors was optically determined to within <0.5 deg. The zero-angle calibration of the angular system was determined to within <1.0 deg. by observing the energy loss in the H(n;n) scattering process at a number of scattering angles both left and right of the zero-scattering-angle center line.

The neutron detectors were hydrogeneous scintillators placed at a flight path of ≈5 m within a large shield system. The relative energy-dependent efficiency of each detector was determined by the observation of neutrons scattered at various angles from hydrogen at a fixed incident energy or by observation of neutrons emitted following the spontaneous fission of ^{252}Cf; or by both methods. The normalization of these relative sensitivity distributions was determined using to the well-known H(n;n) cross section at each incident energy (13). These detector calibration procedures provided a good knowledge of detector sensitivities over the rather wide energy range encountered in scattering from the light nucleus ^{6}Li. The uncertainties associated with the detector sensitivities varied with the particular measurements and energy range but were generally 3 to 5 percent. These uncertainties were a major contribution to the overall cross-section uncertainties. Further details of the detector calibration procedures are given in Refs. 12, 14 and 15.

Thg scattering samples, outlined above, were placed at the focus of the ten time-of-flight collimators approximately 14 cm. from the neutron source. In addition to the ^{6}Li samples and associated empty containers, polyethylene and carbon samples were used at each incident energy. All samples were of the same cylindrical geometry and size as the ^{6}Li samples. The polyethylene sample was employed in the detector sensitivity determinations as outlined above. Cross sections were routinely deduced from the observed scattering from carbon in order to test the fidelity of the instrument. The differential carbon elastic scattering cross sections are well known away from sharp resonance structure and the angle-integral is essentially the well-known total neutron cross section at the energies of the present measurements (11).

Data acquisition was via an on-line digital computer using an 11 x 512 x 16 matrix consisting of; 10 detectors plus monitor, 512 time-channels each, and 16 energy-recoil channels each. Data reduction to cross section proceeded through an integrated data-handling system which include corrections for angular resolution, incident particle attenuation and multiple events. These correction procedures employed both analytical and monte-carlo techniques and were pursued to accuracies of $\lesssim$1 percent with respect to the cross section result. Details of the data processing and correction procedures are to be found in Ref. 12.

IV. Experimental Results

A. Broad-resolution Neutron Total Cross Sections

The broad-resolution neutron total cross sections were measured from $\approx$0.5 to 4.8 MeV during two widely separated measurment periods. The first set employed the two Argonne samples in a tandem arrangement. The second set employed the same tandem arrangement of Argonne samples plus the thicker reference sample obtained from BCMN. The statistical accuracies associated with the cross sections varied from 1 to 4 percent depending upon the particular measurement. The results were generally consistent within the statistical uncertainties with no recognizable dependence on the sample configuration or measurement period. There remained possible systematic uncertainties associated with the samples as outlined above and further discussed in Ref. 5. These were estimated to be 1.0 to 2.0 percent for measurements involving the ANL samples and less for those employing the BCMN sample.

The experimental results are compared with the previously reported BCMN values in Fig. 1 (4). Over the comparable energy range of 0.5 to 3.0 MeV the results from the two laboratories are in very good agreement. An "eye-guide" with $\pm$ 3 percent uncertainty limits was constructed through the results from the two laboratories as illustrated in Fig. 1. A large majority of the measured values lie within the $\pm$ 3 percent "eye-guide" band and more than 66 percent of the values fall within a narrower $\pm$ 2 percent band. The present results can be combined with previously reported values from ANL (5) and from BCMN (4) to obtain a comprehensive knowledge of the neutron total cross section of ^{6}Li from 0.1 to nearly 5.0 MeV as illustrated in Fig. 2. Again, these results appear consistent to within better than the 3 percent band of the "eye-guide" excepting a small energy shift at lower incident energies as discussed in Ref. 5.

The present results can be compared with other previously reported measured and evaluated neutron total cross sections as illustrated in Figs. 3 and 4. The results of Harvey and Hill (16) are in very good agreement with the present results; only one Harvey and Hill point falls beyond the present "eye-guide" $\pm$ 3 percent and that point appears anomolous. The present results are in reasonable agreement with the values of Uttley et al. (3) excepting regions near 1.5 and 3.0 MeV where the latter values appear to lie lower than the present results. The results of Goulding et al. (17) at energies below approximately 3.0 MeV are larger than the present values but in agreement at higher energies. The same general comparative trends are

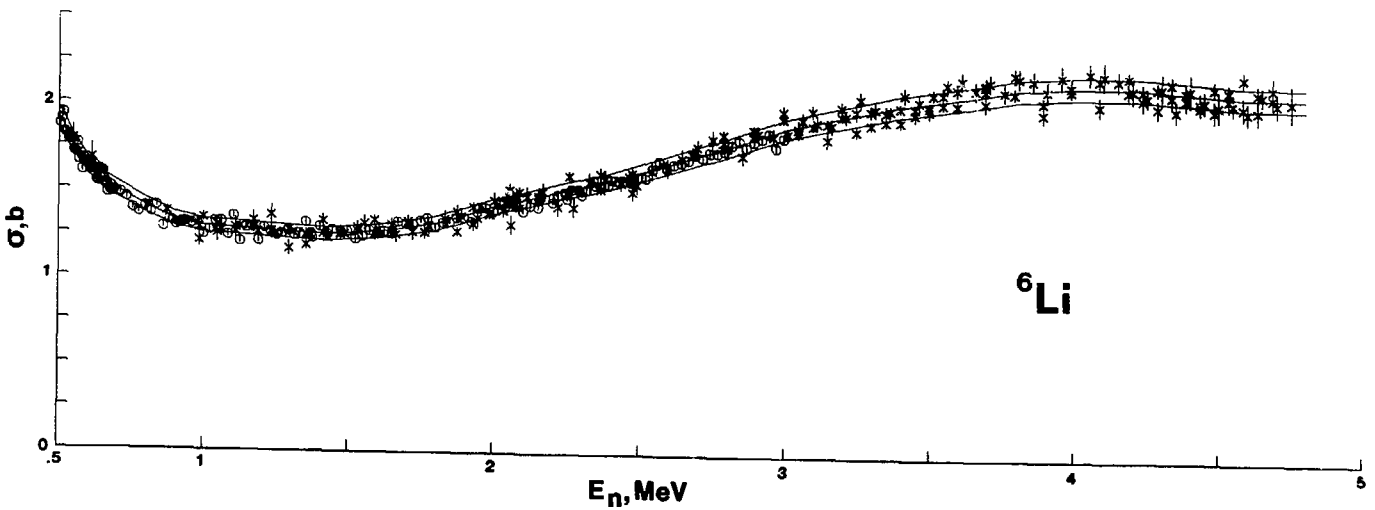

Fig. 1. Measured neutron total cross sections of ^{6}Li. The present results are indicated by (x), those of Ref. 4 by (0) and an "eye-guide" ±3% by the curves.

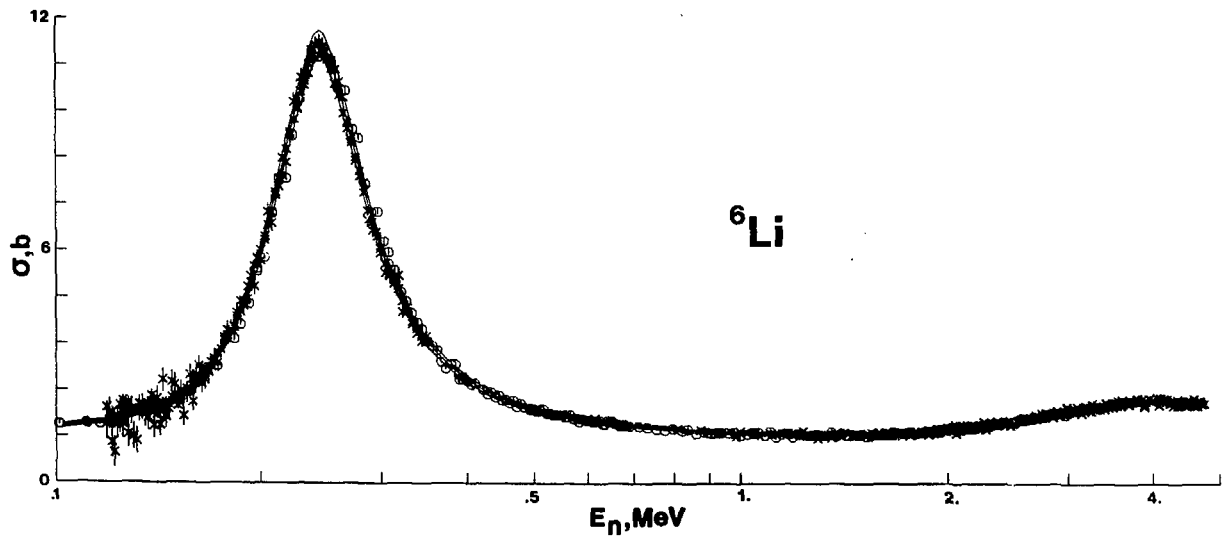

Fig. 2. Measured neutron total cross sections of ^{6}Li from 0.1 to 4.8 MeV. The present results and those of Ref. 5 are indicated by (x), those of Ref. 4 by (O). The curves denote an "eye-guide" ±3%.

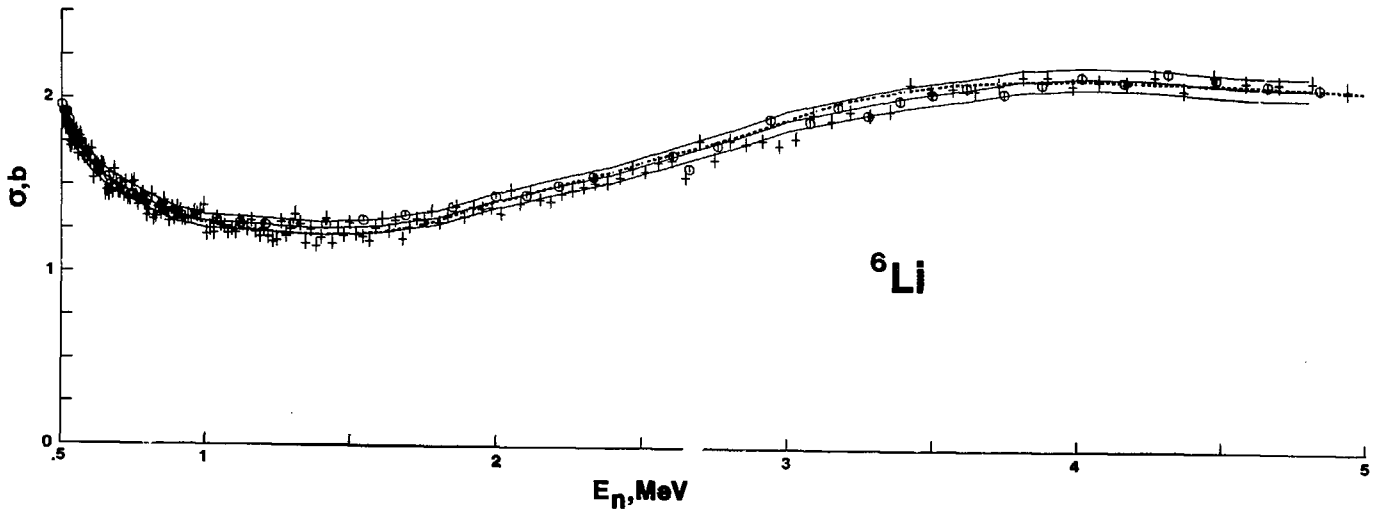

Fig. 3. The "eye-guide" ±3% deduced from the present results (solid curves) compared with the results of Harvey and Hill (0) (16), Uttley et al. (+) (3), and the ENDF/B-V evaluation (dashed curve) (6).

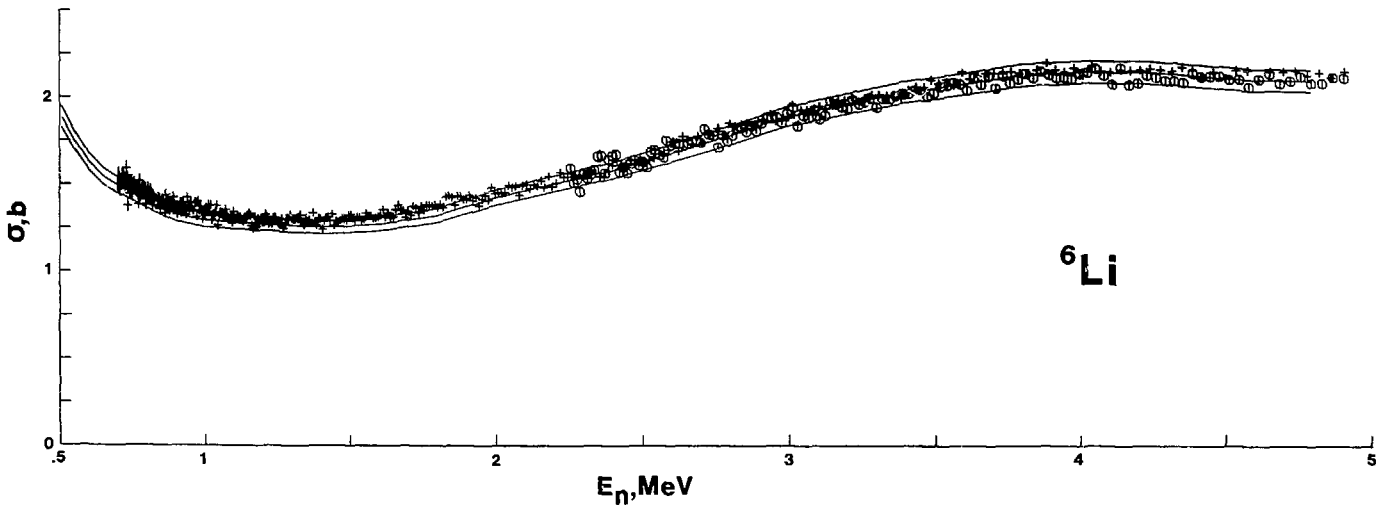

Fig. 4. The "eye-guide" ±3% deduced from the present results (solid curves) compared with the measured values of Goulding et al. (+) (17) and Foster and Glasgow (0) (18).

true with respect to the results of Foster and Glasgow (18). Results reported by Johnson et al. (19) disagree with the present values by 5-10 percent below several MeV. Results of Meadows and Whalen (20) tend to be ≈5 percent higher than the present values near 1.0 MeV. Other available information tends to be too fragmentary to permit a comprehensive comparison.

B. Differential Neutron Scattering Cross Sections

The differential neutron scattering measurements were made at ≲100 keV intervals from 1.5 to 4.0 MeV and at ten or more scattering angles distributed between ≈20 and 160 deg. Incident neutron energy resolutions were 15-30 keV and scattered-neutron velocity resolutions were ample to resolve descrete inelastically-scattered neutron groups resulting from excitations of known states in ^{6}Li. The measurements were made during several experimental periods. When results were obtained at approximately the same incident energy they were averaged.

The elastic-scattering results are outlined in Fig. 5. The accuracies of the individual data values varied from 5-10 percent as discussed in Section III, above. The measured values in the center-of-mass system were fitted with a Legendre polynomial expansion of the form

$$\frac{d\sigma}{d\Omega} = \frac{\sigma}{4\pi}\left[1 + \sum_{\ell=1}^{n} \omega_\ell P_\ell\right] \qquad \text{(IV-1)}$$

($n = 2$ for $E_n \leq 2.0$, $n = 4$ for $E_n > 2.0$ MeV)

using least-square fitting procedures. The resulting polynomial fits generally agreed with the measured values to within the experimental uncertainties. Exceptions were confined to a few isolated experimental values or distributions where the fitting procedures were unduly influenced by values near the extremity of the measured-angular range.

The angle-integrated elastic scattering cross sections follow directly from the above fitting procedures. The results are illustrated and compared with previously reported BCMN results (4) and those of Lane et al. (21) in Fig. 6. The uncertainties attributed to the present angle-integrated values were generally 3-5 percent. There were a few exceptions associated with more uncertain measurements (e.g. at 1.5 MeV). These uncertainty estimates were inclusive of systematic effects particularly those associated with the samples as discussed above. An "eye-guide" with a ± 4 percent uncertainty band encompassed nearly all of the present results as well as those of Refs. 4 and 21, as illustrated in Fig. 6.

The present differential neutron elastic-scattering measurements are in agreement with those by Lane et al. (21) though the latter extend to only ~1.8 MeV. Batchelor and Towle have reported elastic scattering measurements at 3.35 and 4.0 MeV (22). Lane et al. have reported elastic-scattering measurements extending from ~4.0 MeV upward in energy (23). The results of Refs. 4, 22 and 23 are reasonably consistent with the present values as illustrated in Fig. 7 and 8.

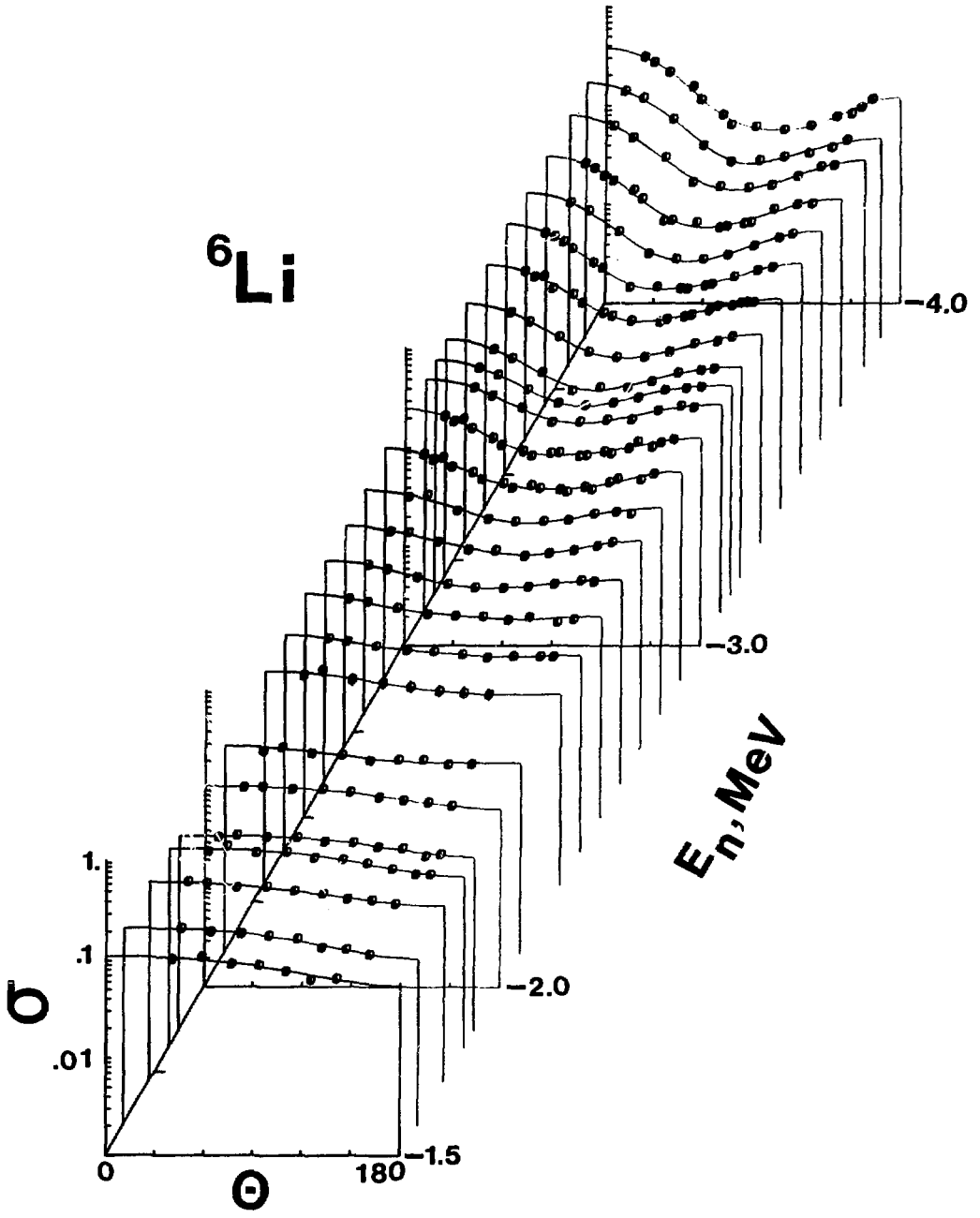

Fig. 5. Summary of the Present Differential-elastic-scattering Measurements. Measured values are indicated by data points and the results of a *Legendre polynomial* fit to the measured values by the curves. The dimensionality is differential cross section in b/sr and scattering angle in center-of-mass degrees.

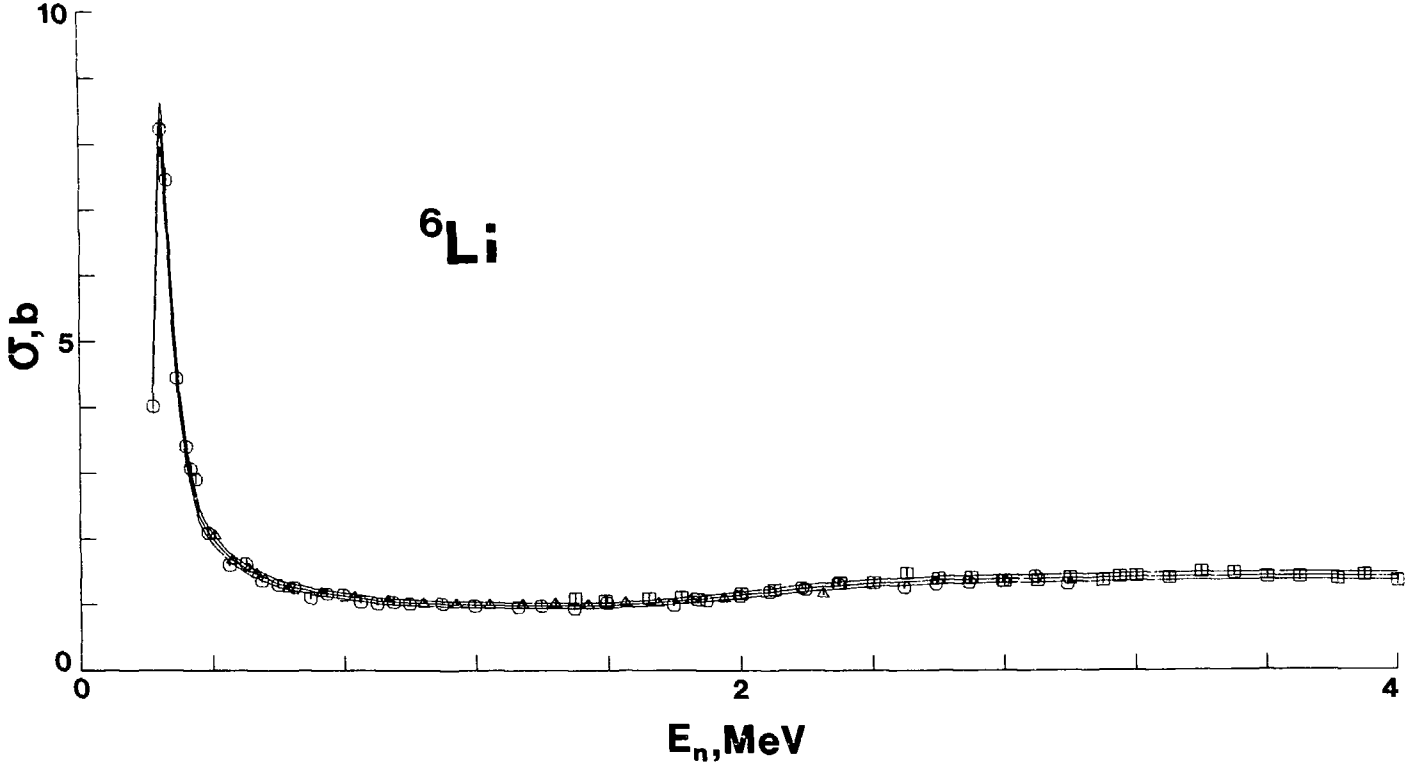

Fig. 6. Angle-integrated elastic neutron scattering cross sections of ^{6}Li. Present results are indicated by □, Ref. 4 by ⊙ and Ref. 21 by △. Curves denote an "eye guide", ±4%.

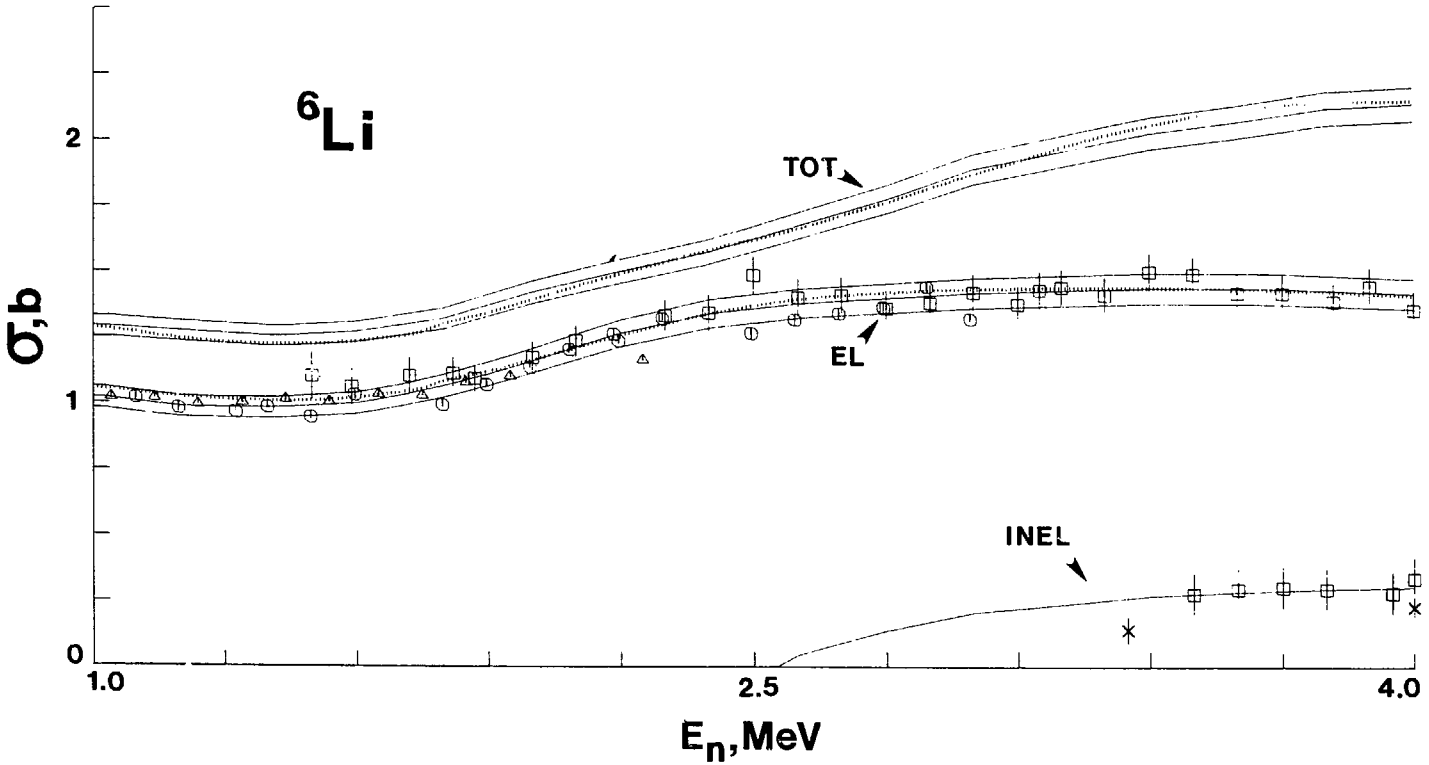

Fig. 7. Measured Neutron Total, Elastic- and Inelastic-Scattering Cross Sections. Present results are indicated by (□), those of Ref. 4 by (○), those of Ref. 2 by (△) and those of Ref. 22 by (x). Solid curves indicate "eye-guides" with ± uncertainty bands including those for the neutron total cross section as defined in the text. The dotted lines denote comparable values as given in ENDF/B-IV.

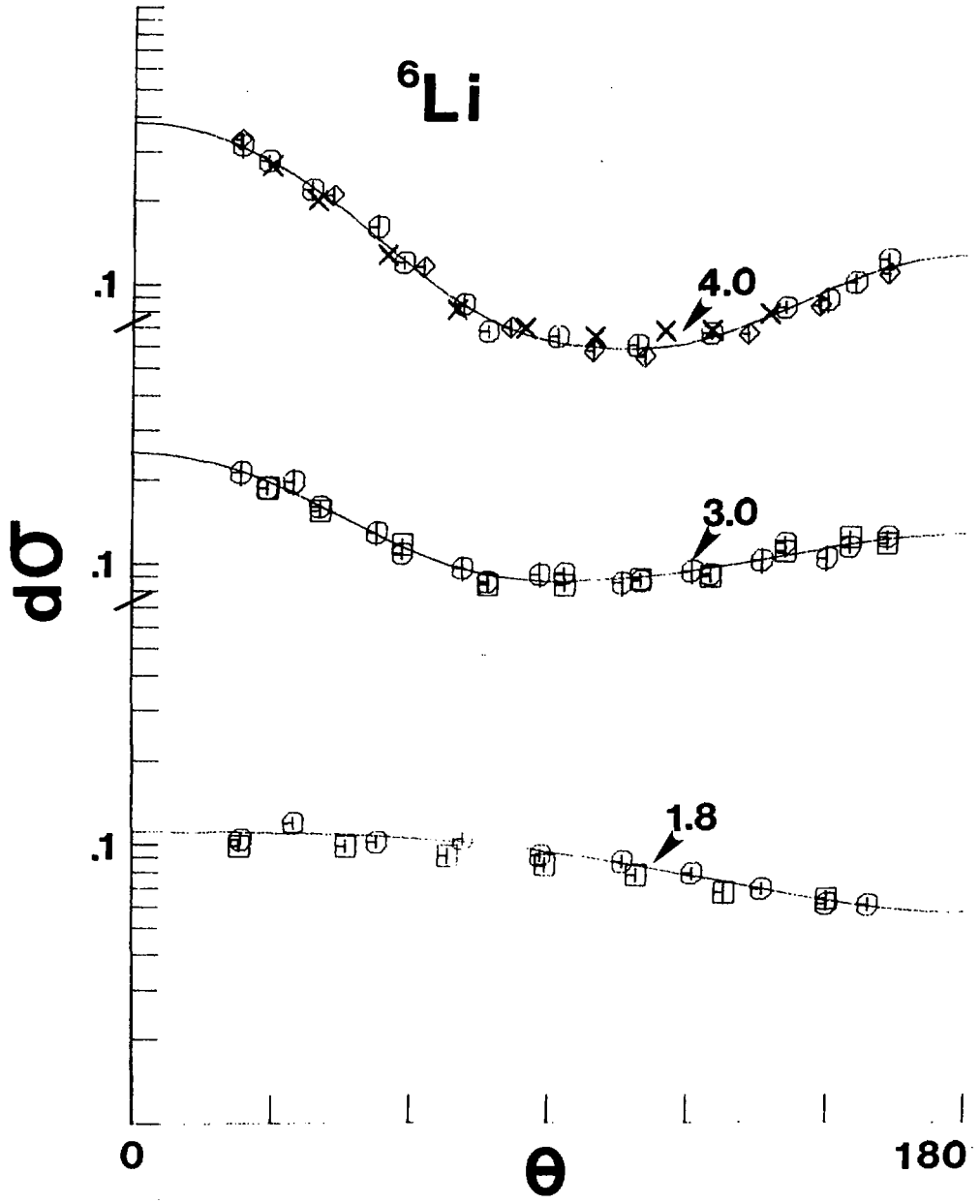

Fig. 8. Select comparisons of measured differential neutron elastic-scattering cross sections. Present results are indicated by (○), those of Ref. 4 by (□) Ref. 23 by ◇, and Ref. 22 by x. Curves indicate Legendre Polynomial fits to the present results.

Inelastically-scattered neutrons corresponding to the descrete excitation of the 2.184 MeV state in ^{6}Li were resolved in the present measurements at higher incident energies and forward scattering angles. The corresponding angle-integrated inelastic scattering cross sections were deduced from the measured values assuming that the neutron emission was isotropic in the center-of-mass system. The resulting angle-integrated cross sections are shown in Fig. 7. The illustrated uncertainties are subjective estimates based upon the quality of the data. The only comparable measurements appear to be those of Batchelor and Towle (22). Those results tend to be somewhat smaller than the values of the present work but not beyond the respective uncertainties.

V. Interpretation and Discussion

A. Qualitative Observations

Over the energy range of the present experiments the n + ^{6}Li reaction has several prominent features. Below ~1.7 MeV the neutron channels and a single alpha-particle channel (^{6}Li(n;α)t, Q = 4.783 MeV) are open and the cross sections are dominated by a large and well isolated 5/2 - resonance at ~0.25 MeV (1). The neutron and alpha-particle widths of this resonance are of the same order of magnitude. At very low energies the (n;α) cross section is relatively large and follows the 1/v energy dependence characteristic of a strong ℓ = 0 contribution. Nuclear-reaction studies have not explicitly identified the corresponding 1/2 + or 3/2 + resonance in relevant bound or unbound energy regions. The neutron-reaction evidence for the ℓ = 0 component is unequivocal but the detailed character remains ambiguous. As incident energies increase above ~1.7 MeV a number of channels rapidly open. The first of these is due to the (n;n′,d)α reaction (Q = -1.421 MeV) and the next to the (n;n′) reaction (Q = -2.185 MeV). The residual 3+ level of ^{6}Li may decay by n-d breakup or descrete gamma-ray emission. The latter process was observed in the present measurements and has a relatively large cross section. The contribution from other high-energy open channels is probably relatively small in the context of the present measurements. Throughout the higher-energy region of the present experiments the relevant ^{7}Li resonance structure is very broad, ill-defined and uncertain. Contemporary understanding of the various channels and their respective neutron cross sections is reasonably summarized in Ref. 6. The present measurements bear upon the n + ^{6}Li reaction in the context of neutron total and scattering cross sections and the present interpretation is based only upon the present experimental values. It was the objective of the interpretation to quanitatively describe the measurements with a simple model employing as few parameters as possible. It was hope that the model would be a suitable vehicle for interpolation within the present experimental context and for extrapolation to channels not measured in the present experiments; in particular the (n;α)t reaction frequently employed as a reference standard at low neutron energies.

B. Basic Concepts

The present interpretation is based upon the nuclear-reaction concepts of Blatt and Biedenharn (24). The nuclear cross sections are expressed in terms of the collision matrix, $U_{cc'}$; where c and c′ are coventional channel

indexes. The $U_{cc'}$ elements are formulated in the context of the R-matrix theory of Wigner and Eisenbud (25); discussed in detail by Lane and Thomas (26). In this formulation

$$U_{cc'} = \Omega_c \, W_{cc'} \, \Omega_{c'} \quad , \tag{V-1}$$

where

$$W_{cc'} = \delta_{cc'} + 2i \, P_c^{1/2} \, P_{c'}^{1/2} \left\{ (1 - R^\circ_{cc} \, L^\circ_{cc})^{-1} \, R^\circ_{cc} \, \delta_{cc'} + \sum_{\lambda\mu} (a_{\lambda c} \, a_{\mu c'}) A_{\lambda\mu} \right\} \tag{V-2}$$

$\Omega_c = e^{-i\phi_c}$

ϕ_c = hard-sphere phase shift

P_c = penetrability

R°_{cc} = background matrix, assumed real and diagonal

$L^\circ_c = S_c - b_c + iP_c$

S_c = shift factor

b_c = boundary conditions assumed equal to S_c at resonance

$a_{\lambda c} = \gamma_{\lambda c}/(1 - R^\circ_{cc} \, L^\circ_c)$

$\gamma_{\lambda c}$ = reduced width of level λ

In the present application a 2-level formulation was assumed. With that assumption (26)

$A_{11} = \varepsilon_2/D, \quad A_{12} = A_{21} = \xi_{12}/D, \quad A_{22} = \varepsilon_1/D$

$\varepsilon_\lambda = E_\lambda - E - \xi_{\lambda\lambda}$ where E and E_λ are energy and resonance energy, respectively.

$D = \varepsilon_1 \, \varepsilon_2 - \xi_{12}^2$

$\xi_{\lambda\mu} = \sum_c (L^\circ_c \, \gamma_{\lambda c} \, \gamma_{\mu c})/(1 - R^\circ_{cc} \, L^\circ_c)$,

the indexes λ and μ running through 1 and 2.

In the present case the above can be reduced to the single-level form with little detriment but the more general 2-level form was used in the present calculations.

The differential neutron cross section is given by

$$\frac{d\sigma_{cc'}}{d\Omega} = \frac{\lambda^2}{(2I + 1)(2i + 1)} \sum_{ss'} \sum_{L=0}^{\infty} B_L \, P_L \, (\cos \theta) \qquad \text{(V-3)}$$

where P_L is the conventional Legendre polynomial and s and s' the channel spins (in this case the target spin (I) = 1, the neutron spin (i) = 1/2 and thus the two channel spins are s = 1/2, s' = 3/2). The B_L are given in terms of geometrical factors and $U^J_{cc'}$ in Ref. 24. The neutron polarizations can be expressed in a manner anolagous to that of Eq. V-3 (27). The angle-integrated neutron cross section is simply proportional to the B_0 term of Eq. V-3. The cross sections for the non-neutron channels are given by

$$\sigma^J_{nx} = \frac{\pi}{\lambda^2} g_J \left| W_{nx} \right|^2 \qquad \text{(V-4)}$$

where g_J is the conventional statistical factor (28).

C. Implementation

The practical calculations used the above concepts assuming neutron orbital angular moments of ≤ 2. This was not believed to be a stringent limitation in the present case. Four reaction channels were considered; two neutron channels (channel spins 1/2 and 3/2), an alpha-particle channel associated with the (n;α)t reaction (Q = 4.783 MeV) and a second alpha-particle channel (Q = - 1.421 MeV). The latter was assumed to represent the intermediate step in the n-d breakup process; i.e. (n;α)t → (n;n',d)α. Other channels with higher-energy thresholds were ignored. Their inclusion would have led to a rapid proliferation in the number of parameters involved and the corresponding cross sections are believed to be relatively small (6). An exception is the (n;n') reaction (Q = - 2.184 MeV), the cross sections of which were observed in the present experiments to be appreciable. The B_L values of Eq. V-3 are proportional to multiple sums over angular momenta

$$B_L \sim \sum_{J_1 J_2} \sum_{\ell_1 \ell_2} \sum_{\ell_1' \ell_2'} Z(\ell_1 J_1 \ell_2 J_2 L) \, Z(\ell_1' J_1 \ell_2' J_2 L) \times$$

$$\left(\delta_{\ell_1 \ell_1'} - U^{J_1}_{\ell_1 \ell_1'}\right)^* \left(\delta_{\ell_2 \ell_2'} - U^{J_2}_{\ell_2 \ell_2'}\right) \quad . \qquad \text{(V-5)}$$

A large number of $U_{cc'}$ elements are generally involved in Eq. V-5 with corresponding parameters. Thus $U_{cc'}$ was assumed diagonal in ℓ; i.e. $\ell_1 = \ell_1'$. A detailed study by Gupta and Shastry support the validity of this assumption in the present context (29) and similar assumptions have been successfully employed elsewhere, e.g. Ref. 30. The assumption was further supported by a simplified version of the present calculations including all $U_{cc'}$ elements in the context of only neutron channels. No significant improvement in the description of the present measured values was achieved at the expense of the introduction of additional parameters.

Initial estimates of resonance properties were taken from the compilation of Ref. 1. A number of modifications and/or alternatives were pursued in the course of the calculations always keeping in mind the objective of simplicity. The calculations were carried out with a relatively small digital computer (32 k of 24 bit words) using various versions of a FORTRAN-IV program developed from a formulation of R. Lane et al. (31). One version was a Xi-square fitting procedure optimizing parameters to best describe the observed neutron total and/or elastic-scattering cross sections. This (and all) versions of the program used, as an additional input, the thermal cross section value for the (n;α)t reaction. The Xi-square fitting was carried out to incident energies of ~1.7 MeV. The resonance widths and energies and the elements of the background matrix were taken as variable parameters. The parameter set obtained from the fitting procedure was "tuned" using a graphical version of the program and subjective judgment to improve the description of measured values, particularly at higher energies where the procedures were certainly only approximations. The finally accepted "general" parameters of Table I constitute very nearly a single-level interpretation. The present parameter set is similar to that of Ref. 30 though somewhat simplier. It does include the fourth (pseudo) (n;n,'d)α channel (Q = -1.421) but the latter contribution is very small and the corresponding parameters uncertain.

D. Comparisons of Calculated, Measured and Evaluated Cross Sections

Calculated and measured angle-integrated cross sections are compared in Figs. 9 and 10. The present experimental values are represented by uncertainty bands derived as outlined in the preceding section. The calculated neutron total cross section is within the ±3% experimental uncertainty throughout the energy range 4 keV to 1.0 MeV (see Fig. 9). The calculated elastic scattering values are within the ±4% experimental band from 0.4 to 1.0 MeV. Below 0.4 MeV the calculated and measured neutron elastic-scattering cross sections are of similar shape but differ in energy scale by 4 to 5 keV. Differential elastic scattering measurements in this area are difficult and small uncertainties in energy scale and/or resolution can easily result in systematic differences of the size observed. The energy scale of the neutron total cross section measurements was believed more reliable and was used in the model calculations. The model parameters, based upon the present neutron total and scattering cross section measurements imply the illustrated (n;α)t cross section.

Figure 10 extends the above comparisons of measured and calculated angle-integrated cross sections to $\gtrsim$4.5 MeV. The elastic scattering cross sections are in very good agreement to the upper limit of the measurements (i.e.

Table I, R-Matrix Parameters[a]

ℓ	$J\pi$	$E_{j\ell s}$	$S^c=1/2$		$S^c=3/2$		$\Gamma^d_{\alpha_0}$	$R^o_{\alpha_0}$	$\Gamma^d_{\alpha_1}$	$R^o_{\alpha_1}$
			Γ_{n_1}	$R^o_{n_1}$	Γ_{n_2}	$R^o_{n_2}$				
0	1/2+	---	---	0.125	---	---	---	---	---	---
0	3/2+	2.25	---	---	3.000	---	0.770	---	---	---
1	1/2-	---	---	---	---	---	---	---	---	---
1	3/2-	4.00	0.300	0.500	4.50	0.200	---	---	1.50	0.200
1[b]	5/2-	0.248	---	---	0.090	0.100	0.035	---	---	---
		-0.752	---	---	0.002	---	0.215	---	---	---

[a]All energies in laboratory MeV, radii $r = 1.4\ (A_1^{1/3} + A_2^{1/3})$;F.

[b]Two levels

[c]Neutron channel spins $S = I \pm 1/2$.

[d]α_o = (n;α) reaction (Q = 4.78 MeV), α_1 = pseudo (n;n´d) reaction (Q = -1.42 MeV).

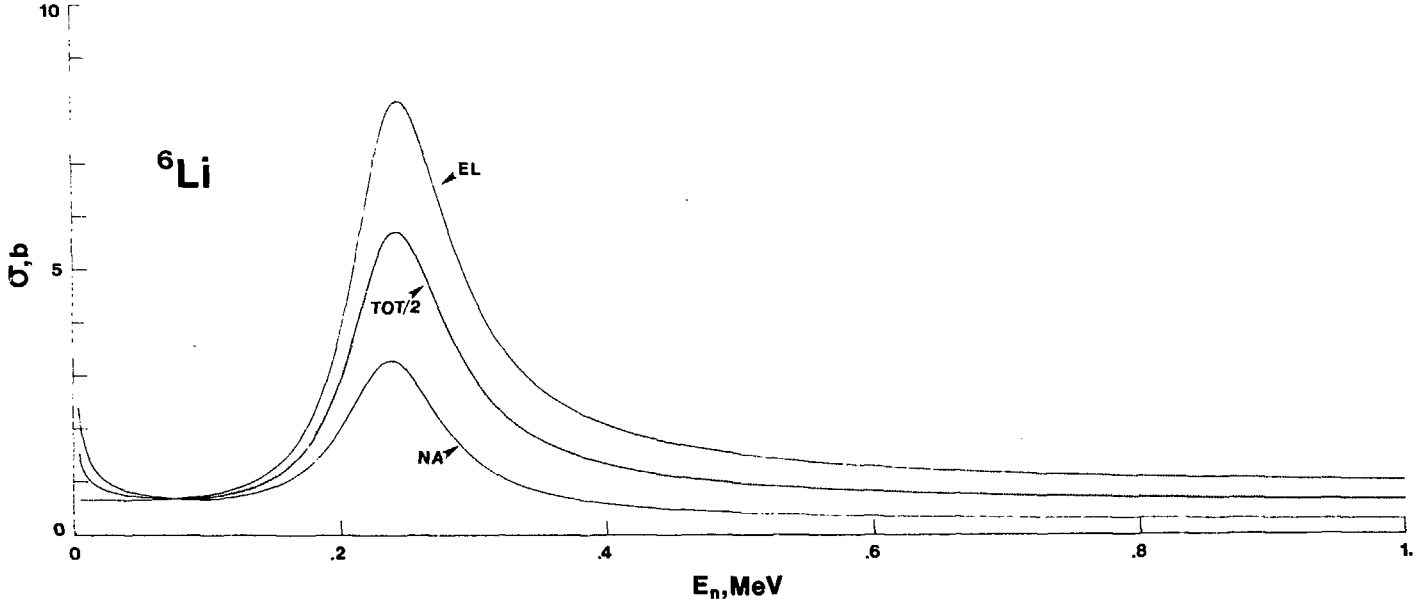

Fig. 9. Comparison of the present measured and calculated neutron total and elstic-scattering cross sections of ^{6}Li over the energy range 4 keV to 1 MeV. Calculated results are noted by solid curves. Dashed lines indicate the experimental results with associated uncertainties as described in the text. The implied (n;α)t cross section is also shown.

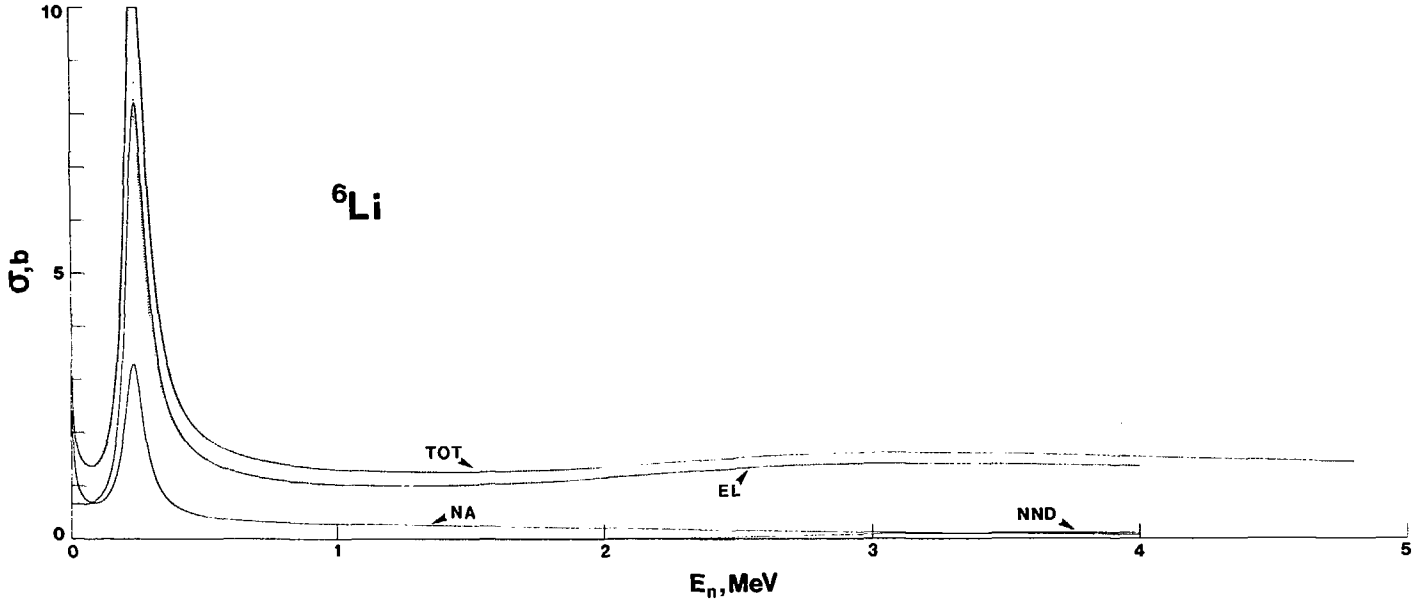

Fig. 10. Comparison of present measured and calculated neutron total and elastic-scattering cross sections of ^{6}Li over the energy range 4 keV to 4-5 MeV. Calculated results are indicated by solid curves and experimental values with estimated uncertainties by dotted bands. The implied $(n;\alpha_o)$ and $(n;n,d_o)$ are also indicated.

4.0 MeV). There is similar good agreement between measured and calculated neutron total cross sections to ~2.5 MeV. At higher energies the measured neutron total cross sections become progressively larger than the calculated values by amounts that are consistent with the contributions from higher-energy channels not considered in the calculations. Most notable of the latter is the $(n;n',\gamma)$ channel (Q = -2.184 MeV) whose cross sections were observed in the present experiments to be of significant size.

Figure 11 illustrates comparisons of measured and calculated differential neutron elastic-scattering cross sections. For these comparisons regions of relatively slow energy dependence were chosen and the experimental data from either BCMN or ANL averaged over energy increments of ±50 to 100 keV in order to smooth experimental fluctuations. At energies of $\lesssim$2.0 MeV the calculations are qualitatively descriptive of the measurements but, quantitatively, the calcualted values tend to be the somewhat larger at large scattering angles. From ~2.0 to 2.5 MeV the agreement is quite good while above 2.5 MeV the calculations tend to be lower than the measurements at large scattering angles. Furthermore, from ~1.3 to 2.0 MeV the observed distributions tend to be convex with angle while those calculated are concave. Similar contrast is evident in previous measurements and calculations; e.g. Refs. 6, 29, 30 and 32. This local situation can be alleviated by parameter adjustment, e.g. by the introduction of a background matrix in the $1/2^-$ channel, as illustrated by the "mod" curve in Fig. 11, but to the detriment of agreement at higher energies. The latter may not be a serious concern in view of the approximations involved at higher energies. However, the parameters of Table 1 were a "general" compromise over the full measured energy range. It is noted that the above problem area is related to the speculative $\ell = 0$ resonance contribution. It is possible that the model is an over simplification of the actual $\ell = 0$ situation.

Previous measurements and interpretations are reasonably represented by the Evaluated Nuclear Data File-B (ENDF/B), version V (6). This File makes extensive use of the R-matrix formalism to interpolate between measured values at energies of <2.0 MeV (33). Thus the File is a good summary vehicle for comparing the present results with a wide spectrum of previous work. The angle integrated cross sections of the File are compared with those calculated in the present work in Figs. 12 and 13. The present calculated neutron total cross section is in very good agreement with that of the File for energies of $\lesssim$2.5 MeV. The only significant differences are at the very peak and on the low-energy side of the ~250 keV resonance. These differences can be entirely attributed to small differences between the present experimental neutron total cross sections and the data base underlying the File. Above ~2.5 MeV the File neutron total cross sections remain in good agreement with the present measurements but systematically exceed the present calculated values by an amount consistent with the contributions from higher-energy channels not included in the calculations.

The neutron elastic-scattering cross sections of the File are similarly in good agreement with the present measurements and calculations over the full energy range of the present work excepting only the region below ~0.4 MeV, as discussed above. The present work implies a $(n;\alpha)t$ cross section (Q = +4.783 MeV) in remarkably good agreement with that of the File despite the fact that the present work is essentially entirely based upon the present measurements

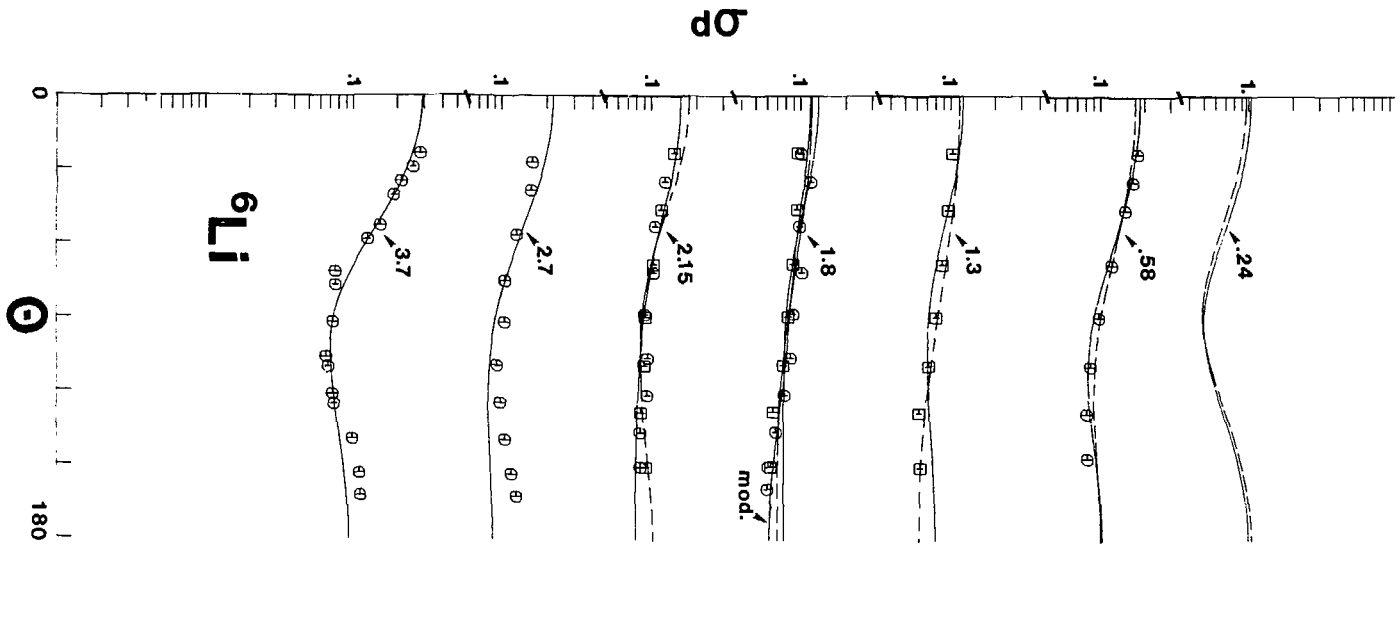

Fig. 11. Comparison of measured, calculated and evaluated neutron elastic-scattering distributions of ^{6}Li. The present experimental results are indicated by ◯ data points, those of Ref. 4 by □. Solid curves indicate the results of the present calculations with alternate parameter sets as discussed in the text. Dotted curves indicate the respective values taken from ENDF/B-V (6). Incident energies are numerically noted in MeV. Differential cross section is given in units of b/sr as a function of scattering angle in degrees in the center-of-mass system.

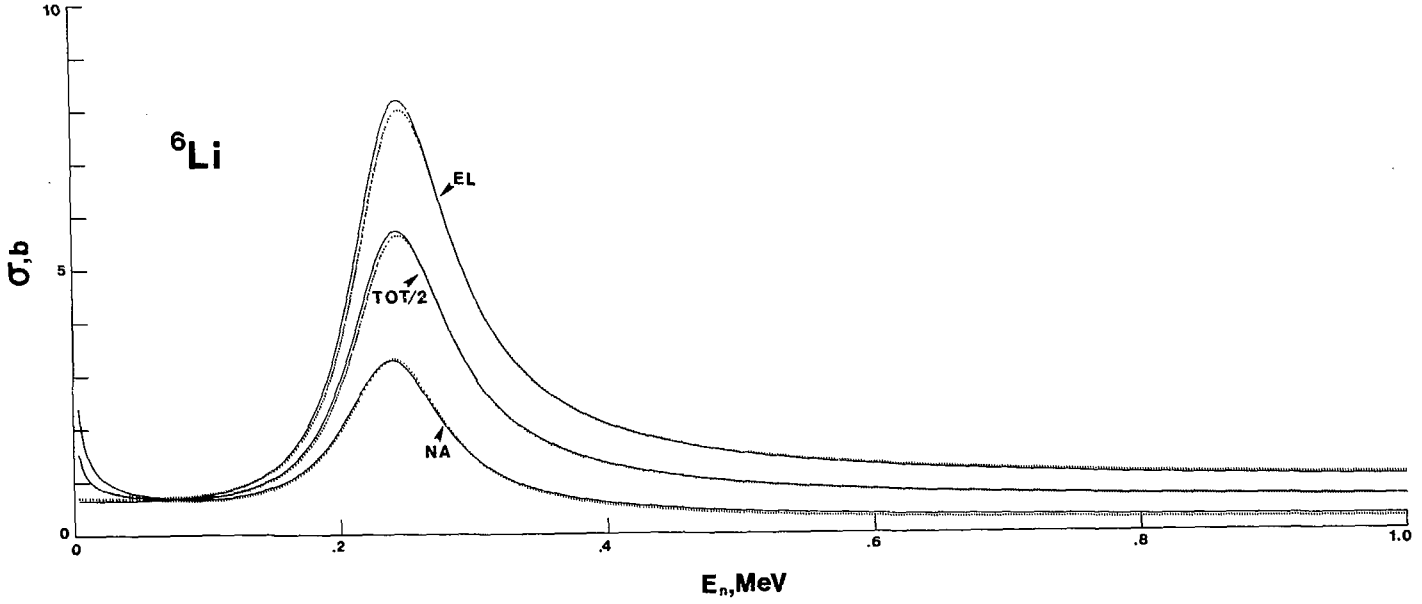

Fig. 12. Comparison of the present calculated cross sections (solid curves) with corresponding values given in ENDF/B-V (dotted lines) over the energy range 4 keV to 1.0 MeV (6).

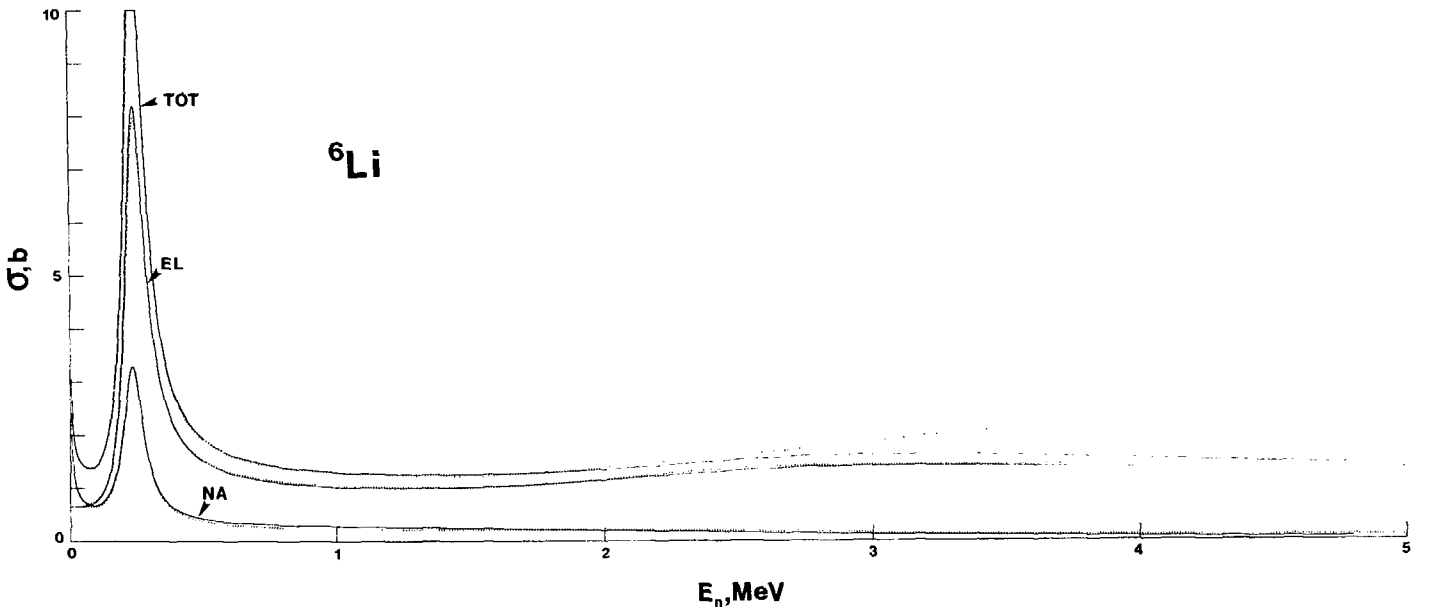

Fig. 13. Comparison of the present and calculated cross sections (solid curves) with values given in ENDF/B-V (dotted lines) over the energy range 4 keV to 4-5 MeV (6).

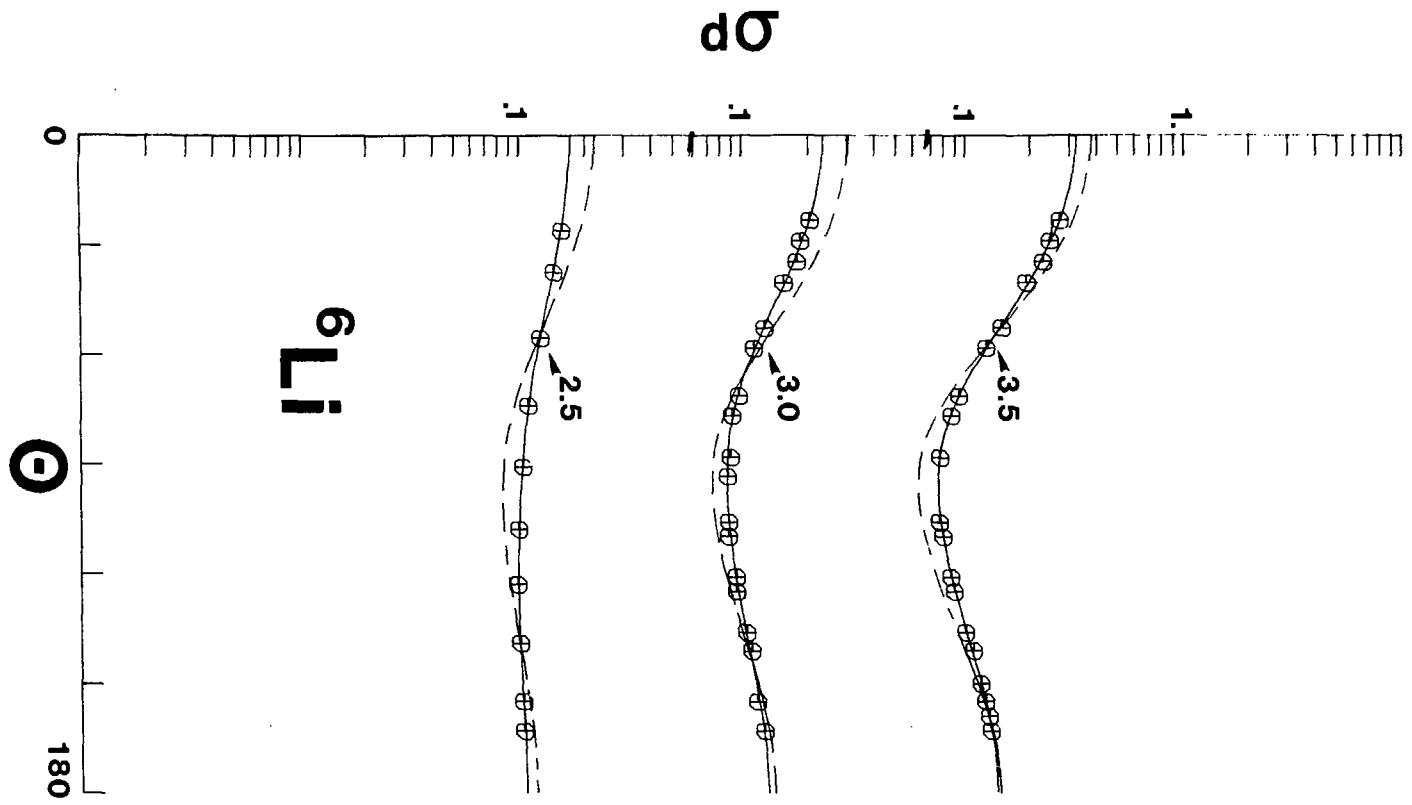

Fig. 14. Comparison of the present measured differential elastic-scattering distributions with those given in ENDF/B-V. The present measured values are noted by data points and corresponding solid curves obtained by fitting the measured quantities with Legendre Polynomial expansions. The corresponding ENDF/B-V (6) distributions are noted by dashed curves. Differential cross sections are expressed as b/sr as a function of center-of-mass scattering angle in degrees. Incident energies are numerically given in MeV.

of neutorn total and elastic-scattering cross sections. The present calculations imply an $(n;\alpha)t$ peak energy ~1.5 keV lower than given by the File and a peak magnitude 0.7% lower. These are very small differences easily attributed to variations in the data bases underlying the two calculations.

Selected portions of Fig. 11 compare the present calculated results at energies of $\lesssim$2.0 MeV with the neutron differential elastic-scattering cross sections of the File. In this energy range both sets of results are directly based upon R-matrix interpretations. The two sets of calculated results are very similar despite their independence and, indeed, different calculational formalisms. Both interpretations appear more representative of the measured values than other similar attempts; e.g. see Refs. 29 and 30.

Figure 14 compares the present measured differential neutron elastic-scattering cross sections with those of the File at energies >2.0 MeV where the latter is apparently an emperical construction from available experimental information. The agreement is only qualitative with the File tending toward greater anisotropy. This is not surprising in view of the limited extent of the previously available data base in this higher energy range.

Neutron polarizations were not a consideration in the present work. However, they were calculated at selected energies using the parameters of Table I. the results were reasonably consistent with the experimental values reported in Ref. 30. This is not surprising as the present parameters and model are qualitatively similar to those of Ref. 30.

VI. Summary

The results of the present experiments provide new knowledge in a hereto-fore uncertain region and suggest some changes in the data base widely used in technological applications (particularly in the area of differential-neutron elastic-scattering cross sections). A simple R-matrix interpretation of the present work and that previously reported by the authors is descriptive of the measured values over wide energy regions and implies an $(n;\alpha)t$ reaction cross section similar to that recommended as a neutron standard (6). However, there remain some outstanding questions. The low-energy $(n;\alpha)$ channel is dominated by an $\ell = 0$ component. The present interpretation, like others (33), associates this component with a positive-energy resonance with a 3/2 channel spin. No such $\ell = 0$ resonance with channel spins 1/2 or 3/2 or positive or negative energies has been explicitly identified in the ^{7}Li system or in the mirror ^{7}Be system. Moreover, the 3/2 channel spin is not consistent with the results of low-energy polarization measurements which suggest that the primary strength is in the channel spin 1/2 channel (34,35). Even the qualitative features of the reaction mechanisms are uncertain as Weigmann and Manakos (36) have recently suggested that the low-energy ^{7}Li$(n;\alpha)$ reaction is governed by a direct deuteron-exchange mechanism rather than the resonance processes assumed above. Other areas of uncertainty are associated with excitations in the few-MeV region. Numerous channels are energetically open but their respective cross sections are uncertain and difficult to measure partly due to the breakup nature of the processes. Throughout this higher-energy region the underlying resonance structure remains broad, ill-defined and with uncertain parameters.

ACKNOWLEDGEMENTS

The authors are indebted to R. Holt, G. Hale, H. Knitter and R. Lane for helpful suggestions and criticism over an extended period of time. We also are particularly indebted to R. Lane and H. Knox for generously providing the framework from which the computational procedures of this work were developed and to J. Monahan for helpful guidance particularly with respect to methods of numerical analysis.

REFERENCES

1. F. Solove and T. Lauritsen, Nucl. Phys., A227 54(1974).

2. CINDA, An Index to the Literature on Microscopic Neutron Data, IAEA Press, Vienna (1979).

3. C. Uttley, M. Sowerby, B. Patrick and E. Rae, Sym. on Neutron Standards and Flux Normalization, AEC Symposium Series #23, (1971).

4. H. Knitter, C. Budtz-Jørgensen, M. Mailly and R. Vogt, Neutron Total and Elastic-Scattering Cross Sections in the Energy Range from 0.1 to 3.0 MeV, EURATØM Report, EUR-5727e (1977).

5. A. Smith, P. Guenther, D. Havel and J. Whalen, Note on the 250 keV Resonance in the Total Neutron Cross Section of ^{6}Li, Argonne National Laboratory Report, ANL/NDM-29 (1977).

6. Evaluated Nuclear Data File-B, (ENDF/B) National Nuclear Data Center, Brookhaven National Laboratory. Version IV is outlined in Brookhaven National Laboratory Report, ENDF-200 (1974). Version V is available in numerical form; evaluators G. Hale, L. Stewart, and P. G. Young, MAT-number 1303 (1979).

7. S. Cox and P. Hanley, Bull. Am. Phys. Soc., 60 121(1971).

8. J. Gibbons and H. Newson, Fast Neutron Phys., Vol. 1, Eds. S. Marion and J. Fowler, Interscience Pub., N.Y. (1963).

9. D. Miller, Fast Neutron Phys., Vol. 2, Eds. J. Marion and J. Fowler, Interscience Pub., N.Y. (1963).

10. S. Cierjacks, P. Forti, D. Kopsch, L. Kropp, J. Nebe and H. Unfeld, High-resolution Total Neutron Cross Sections, between 0.5 and 30 MeV, Karlsruhe Report, KKFK-1000 (1968).

11. A. Smith, R. Holt and J. Whalen, Neutron Scattering from ^{12}C in the Few-MeV Region, Argonne National Laboratory Report, ANL/NDM-43 (1978).

12. P. T. Guenther, Elastic and Inelastic Neutron Scattering from the Even Isotopes of Tungsten, University of Illinois Thesis, (1977).

13. J. Hopkins and G. Breit, Nucl. Data, A9 137(1971).

14. P. Guenther, A. Smith and J. Whalen, Phys. Rev., C12 1797(1975).

15. A. Smith, P. Guenther and R. Sjohlom, Nucl. Instr. and Methods, 140 397(1977).

16. J. Harvey and N. Hill, Proc. Conf. on Nucl. Cross Sections and Technology, National Bureau of Standards Pub., NBS-425 (1975).

17. C. Goulding, J. Clement and P. Stoler, Chicago Operations Office Report, COO-3058 (1972); Data available from the National Nuclear Data Center, Brookhaven National Laboratory.

18. D. Foster and D. Glasgow, Phys. Rev., C3 576(1971).

19. C. Johnson, H. Willard and J. Bair, Phys. Rev., 96 985(1954).

20. J. Meadows and J. Whalen, Nucl. Sci. and Eng., 48 219(1972).

21. R. Lane, A. Langsdorf, J. Monahan and A. Elwyn, Tables of Differential Cross Sections for Scattering of Neutrons from Various Nuclei, Argonne National Laboratory Report, unpublished (1964).

22. R. Batchelor and J. Towle, Nucl. Phys., 47 385(1963).

23. R. Lane, R. White and H. Knox, Proc. Inter. Conf. on the Interaction of Neutrons with Nuclei, CONF-760715 (1976).

24. J. M. Blatt and L. C. Biedenharn, Rev. Mod. Phys., 24 258(1951).

25. E. P. Wigner and L. Eisenbud, Phys. Rev., 72 29(1947).

26. A. M. Lane and R. G. Thomas, Rev. Mod. Phys., 30 257(1958).

27. A. Simon and T. A. Welton, Phys. Rev., 90 1036(1953).

28. Neutron Cross Sections, Vol. 1, 3rd edition, S. Mughabghab and D. Garber, Brookhaven National Laboratory Report, BNL-325 (1973).

29. M. C. Gupta and C. S. Shastry, Phys. Rev., C15 1244(1977).

30. R. J. Holt, F.W.K. Firk, G. T. Hickey and R. Nath, Nucl. Phys., A237 111(1975).

31. R. O. Lane et al., private communication, (1977).

32. R. O. Lane, A. J. Elwyn and A. Langsdorf Jr., Phys. Rev., B136 1710(1964); Numerical values are given in Ref. 21 above.

33. G. M. Hale, National Bureau of Standards Publication, NBS-493 (1977).

34. H. Marshak as quoted in Ref. 3 above.

35. H. Glättli, A. Abragam, G. Bacchella, M. Fourmond, P. Meriel, J. Piesvaux and M. Pinot, Phys. Rev. Lett., 40 748(1978).

36. H. Weigmann and P. Manakos, Z. Phys., A289 383(1979).